Chapter 8 Thunderstorms

"... in the mad thunder-cloud, as when
Fierce legions clash ..."[200]

The previous chapter considered certain dynamical aspects that are basic to all convective clouds. Buoyancy, pressure perturbation, entrainment, and cloud vorticity were introduced and examined, and we noted how these dynamics are incorporated into cloud models. In this chapter, we focus specifically on one type of convective cloud—the cumulonimbus, or thunderstorm cloud. As noted in Chapter 1, cumulonimbus can occur either in isolation (Sec. 1.2.2.1) or as part of large mesoscale convective systems (Sec. 1.3.1). The next chapter of this book is devoted entirely to the structure and dynamics of mesoscale convective systems. Here we will concentrate on the properties of isolated thunderstorms and lines of thunderstorms. An understanding of individual storms and lines is crucial because they are important weather-producing phenomena in their own right and because they are building blocks of the larger mesoscale systems.

The isolated cumulonimbus is one of the most visually striking and photogenic of all cloud phenomena. The visual appearance of these clouds was illustrated by Figs. 1.4 and 1.5. In this chapter, however, we are not concerned so much with the exterior appearance of these clouds as with their internal structure and dynamics. We will begin by examining small, isolated cumulonimbus (Sec. 8.1). Then we will consider larger isolated thunderstorms, which are divided into two categories referred to as *multicell* and *supercell* thunderstorms (Secs. 8.2–8.6). In Secs. 8.8–8.10, we will examine three important circulation features of large thunderstorms: *tornadoes*, *gust fronts*, and *downbursts*. Finally, in Sec. 8.11, we will consider the conditions that favor the grouping of individual thunderstorms into *lines of storms*.

8.1 Small Cumulonimbus Clouds

It is possible for a warm cumulus cloud (i.e., one with no ice in it) to precipitate and hence to be classified as cumulonimbus. Such small precipitating cumuliform clouds are common in the tropics. However, most cumulonimbus clouds contain

[200] Goethe's reference to a thunderstorm.

ice. One of the primary distinguishing features of cumulonimbus (Sec. 1.2.2.1) is that its upper portion is usually composed of ice and is spread out in the shape of a smooth, fibrous, or striated anvil, while its lower portion exhibits the form of a mountain of bulbous towers. This basic structure is seen in both the smallest and largest of cumulonimbus clouds. An empirical model of the dynamical and microphysical structure of a very small, isolated cumulonimbus cloud is shown in Fig. 8.1. This picture, synthesized from some 90 research flights through cumuliform clouds, shows that the cumulonimbus has a younger, developing side and an older, glaciated side. The developing side of the cloud is characterized by updraft motion. In this region are several strong, buoyant updraft cores. At the top of each updraft core is a cloud *turret* ~1–3 km in horizontal dimension. Within the turret the air overturns in the manner of a thermal (Figs. 7.8 and 7.9), where horizontal vorticity is generated to the side of a positively buoyant updraft core (Fig. 7.22a). Superimposed on each turret are spherical *tufts* ~100–200 m in diameter, where smaller-scale overturning produces entrainment of environmental air (Sec. 7.3). Across the cumulonimbus, the tops of the turrets are found at increasingly higher altitudes since the new updrafts form systematically on the developing side of the cloud. The tallest turret in Fig. 8.1 has reached above the 0°C level and attained sufficient maturity that some droplets have grown to sizes exceeding 20 μm. The conditions are thus right for ice enhancement to occur (Sec. 3.2.6). Large concentrations ($\geq 1\ \ell^{-1}$, often ~100 ℓ^{-1} or more) of ice particles appear within minutes of the time that the turret reaches its maximum height. The exact mechanism of enhancement [see hypotheses (i)–(iv) listed in Sec. 3.2.6] is not known. The high concentrations appear first in highly localized regions ~5–25 m wide, within the tufts. The ice particles then extend vertically through the cloud in strands of ice, which at lower levels in the cloud may be in the form of graupel. The strong updraft velocities in the cumulonimbus favor high condensation rates. The copious supercooled water condensed in the updrafts is collected by ice particles to produce the graupel. The heavier ice particles fall through the decaying updrafts and may appear as striations in the precipitation below cloud base. Smaller ice particles are carried upward and laterally outward to form the anvil portion of the cloud, which generally contains the maximum concentrations of ice particles, and where the strand structure is no longer apparent. As the ice particles in the more homogeneous anvil slowly fall out, they aggregate just above the 0°C level. The particles then melt and fall to the earth's surface in the manner of stratiform rain.

The small isolated cumulonimbus illustrated in Fig. 8.1 is sometimes called a *single-cell thunderstorm*, since it usually develops just one main precipitation shower. After the updrafts cease forming, this shower dissipates in the manner suggested by Fig. 6.16. At the end of the life cycle, all that remains is the relatively light precipitation from the anvil, which has a stratiform appearance, with a bright band at the melting level.

The radar-echo life cycle of a single-cell thunderstorm is illustrated by the example in Fig. 8.2. The similarity to the schematic life cycle in Fig. 6.1b is evident. The reflectivity increases and develops into a vertical core at 1818 GMT. It then evolves into a stratiform structure with a bright band at the melting layer.

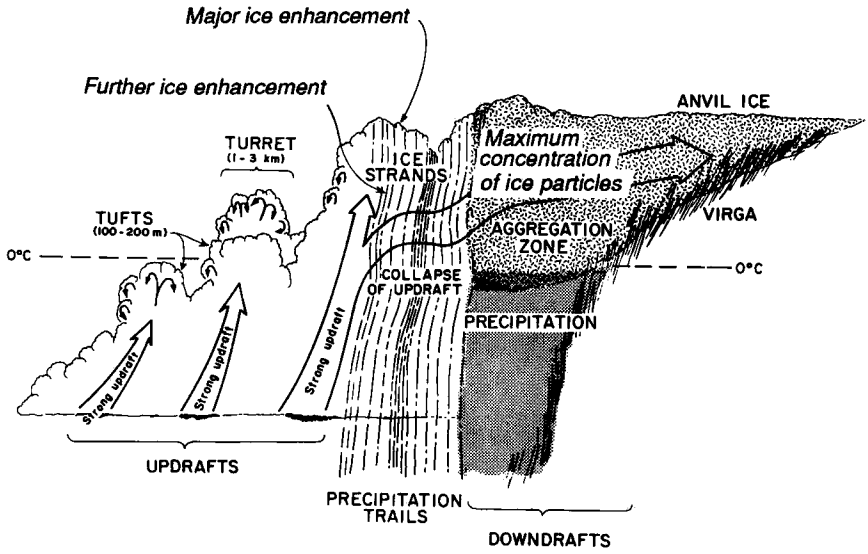

Figure 8.1 Empirical model of a small cumulonimbus cloud. Based on about 90 research aircraft penetrations of small cumulonimbus and large cumulus clouds. (From Hobbs and Rangno, 1985. Reprinted with permission from the American Meteorological Society.)

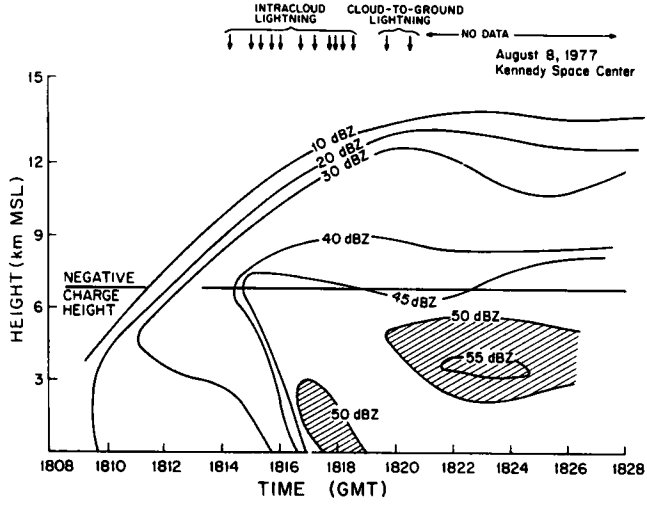

Figure 8.2 Time–height section of radar reflectivity for a thunderstorm near Cape Kennedy, Florida. Times of intracloud (IC) and cloud-to-ground (CG) lightning are indicated. (From Williams *et al.*, 1989. © American Geophysical Union.)

Also indicated in the figure is the sequence of lightning strikes produced by the cumulonimbus. The sequence is rather typical. Frequent lightning does not occur until cloud top rises above the −15 to −20°C level (about 7 km in Fig. 8.2). Intracloud (IC) lightning occurs first and at high frequency for several minutes, especially while the cloud and radar echo are still growing. Cloud-to-ground (CG)

lightning activity (less frequent than IC) tends to lag the IC peak by 5–10 min and occurs after the radar echo contours become flat or, in some cases, begin to descend with time.

The lightning is a manifestation of the fact that the storm is electrified (i.e., positive and negative charges become separated within the region of cloud and precipitation, such that some regions have a net positive charge, while other regions have a net negative charge). The lightning itself is the transfer of charge from one region of a cloud to another or between the cloud and the earth.[201] The narrow channel within which the flash of lightning occurs is heated suddenly to ~30,000 K, with essentially no time to expand. The pressure in the channel is raised by an order of magnitude or two. The high-pressure channel then expands rapidly into the surrounding air and creates a shock wave (which travels faster than the speed of sound) and a sound wave. The latter is the audible signal that one hears as thunder and gives the cumulonimbus its various common names—thunderstorm, thundercloud, thunderhead, thundershower, etc.

The typical distribution of charge within a cumulonimbus is illustrated in Fig. 8.3. The main negatively charged region is sandwiched between two positively charged regions, of which the upper one is larger.[202] The main negative charge zone is notably pancake shaped, tending to be <1 km thick while extending horizontally over several kilometers or more. It is located at a level where the temperature is ~ −15°C. Negative charge is also found in a thin layer surrounding the upper part of the cumulonimbus, including the anvil.

This upper zone is thought to be produced when cosmic-ray-generated negative ions in the environment are attracted to the upper positive region of the cumulonimbus. The ions attach to small cloud particles at the edge of the cloud and form a *screening layer*. The main negative charge causes point discharge or corona from trees, vegetation, and other pointed or exposed objects on the ground below the storm, which leaves positive charge in the atmosphere above the earth's surface.

The mechanisms by which the cumulonimbus becomes electrified remain speculative and an active area of research.[203] One mechanism that appears to be important is the transfer of charge that occurs when graupel particles produced in the region of strong updraft collide with smaller ice particles. It has been demonstrated in laboratory experiments[204] that the polarity of the charge transfer in the collisions is dependent on temperature and liquid water content. Below a critical

[201] For a brief discussion of the physics of the lightning, see Wallace and Hobbs (1977, pp. 206–209).

[202] The inference of the distribution of electric charge in a thunderstorm has a colorful history. It first intrigued the American revolutionary and scientist Benjamin Franklin in the late eighteenth century. In the early twentieth century it gained the attention of the English Nobel laureate C. T. R. Wilson, who is credited with first identifying the dipole constituted by the main negative region in the middle of the cumulonimbus and the main positive region in the upper part of the cloud.

[203] For reviews of the state of knowledge of mechanisms involved in thunderstorm electrification, see Krehbiel (1986), Beard and Ochs (1986), and Williams (1988).

[204] See Sec. 3 of Williams (1988) for a review of these experiments.

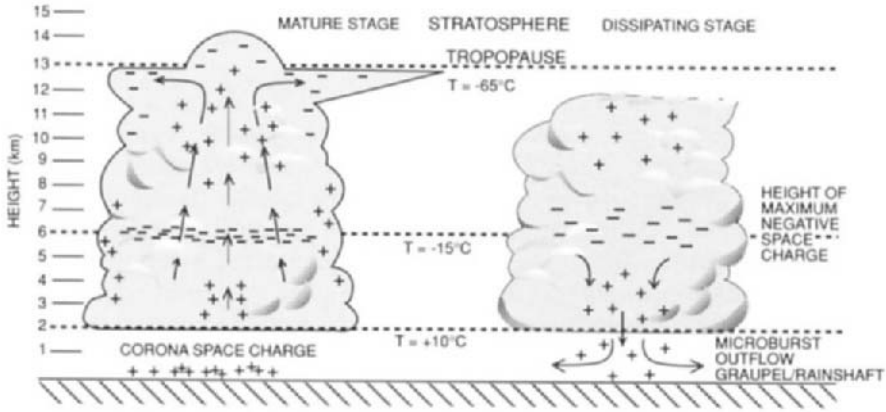

Figure 8.3 Schematic of the electrical structure of a cumulonimbus cloud. Positive and negative signs indicate the polarity of the charge at various locations. Streamlines indicate direction of airflow. (From Williams, 1988. © Scientific American, Inc. All rights reserved.)

temperature in the range -10 to -20°C, called the *charge-reversal temperature*, negative charge is transferred to the graupel, while in warmer air positive charge is transferred.*

The charge reversal temperature has been invoked to explain the distribution of charge depicted in Fig. 8.3, in which the main negative charge zone at ~ -15°C is located between upper-level and lower-level regions of positive charge. According to the *precipitation hypothesis,* the falling graupel particles account for this structure as follows. In the cold upper levels, the graupel particles take on negative charge and leave behind a cloud of small nonfalling particles, which become positively charged when negative charge is transferred to the graupel during collisions. The lower part of the cloud becomes dominated by the negative charge of the graupel particles descending from upper levels—hence the layer of negative charge near -15°C. Below this layer the graupel particles begin to take on positive charge during collisions.

An alternative explanation for the positive charge region at upper levels is the *convection hypothesis,* according to which the upper region of positive charge is accounted for by upward transport of positive charges released into the planetary boundary layer from the earth's surface from the subcloud layer to high levels by the updrafts. Which of these two hypotheses actually applies, under which conditions one is preferred over the other, or how the two may fit together in a common explanation of the charge distribution in a thunderstrom remains uncertain.

* The role of liquid water in the charge reversal is a topic of current research (Takahashi, 1978; Saunders, 1991).

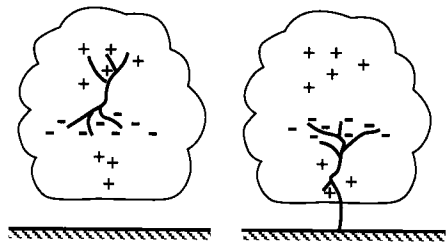

Figure 8.4 Depiction of lightning in prototype electrostatic structures: (a) intracloud; (b) cloud-to-ground. Positive and negative signs indicate the polarity of the charge at various locations. (From Williams *et al.*, 1989. © American Geophysical Union.)

The IC lightning in the earlier stages of the cumulonimbus transfers negative charge from the main negative region to the upper positive zone (Fig. 8.4a). The CG lightning, which comes later, during the mature stage of the storm, usually transfers charge from the main negative region to the ground (Fig. 8.4b). More rarely, positive charge is transferred to the ground.

There are reports of lightning from tropical warm cumulonimbus (i.e., clouds containing no ice).[205] However, this phenomenon does not appear common, and researchers presently regard warm-cloud lightning as the result of some different mechanism than that which electrifies cold clouds.

8.2 Multicell Thunderstorms

The single-cell thunderstorm described in Sec. 8.1 may actually be the most common type of thunderstorm, especially if every towering cumulus that reaches considerable height and precipitates even a small amount is considered to be a thunderstorm. However, the significance of single-cell storms in terms of precipitation or storm damage (other than lightning) is relatively small.[206] The single cell of cumulonimbus takes on more importance when it serves as a building block of a larger *multicell thunderstorm*. The internal structure of the multicell thunderstorm was revealed in the first modern field project designed for intensive storm documentation. It was called the "Thunderstorm Project" and was carried out over 40 years ago. The results of this project, which was the first to employ simulta-

[205] See Moore (1976).

[206] The minor role of single-cell thunderstorms as opposed to multicell storms was addressed by Simpson *et al.* (1980) in relation to precipitation production and by Chisholm and Renick (1972) in connection with storm damage.

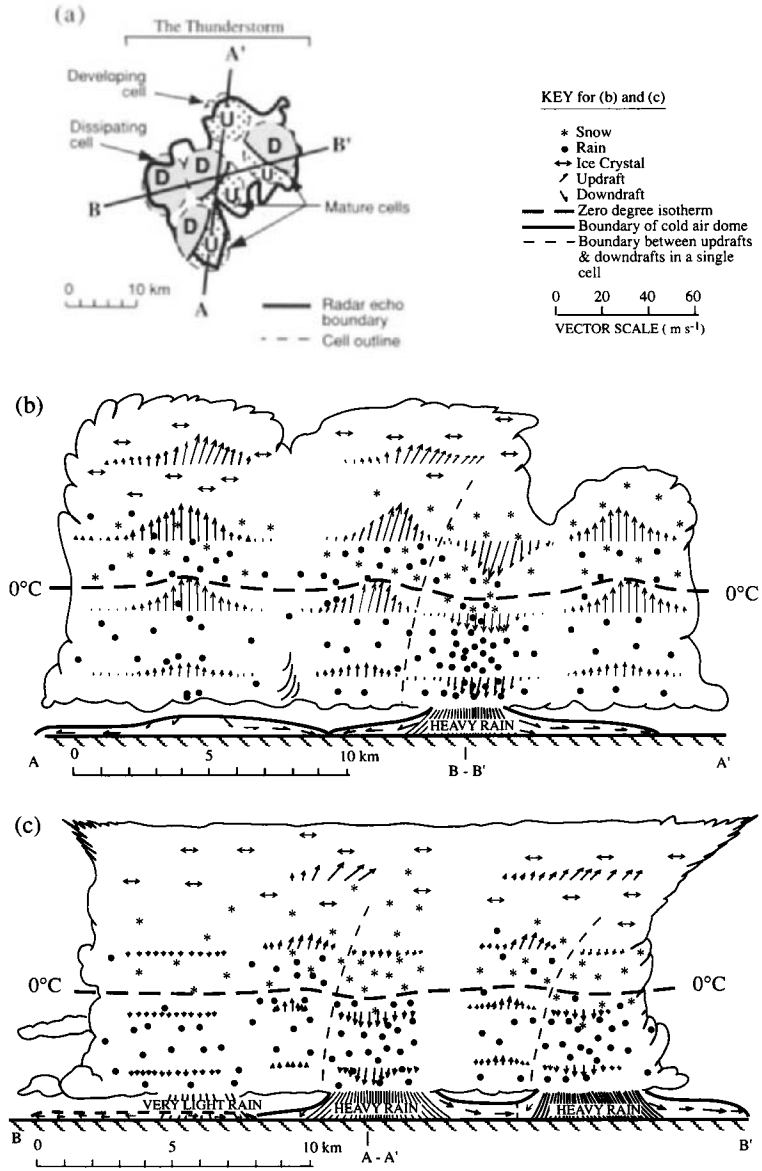

Figure 8.5 Schematic of a multicell thunderstorm in Ohio observed in the Thunderstorm Project. The storm consisted of cells in various stages of development. (a) Plan view. (b) Vertical cross section along A–A′. (c) Vertical cross section along B–B′. (From Byers, 1959. Reproduced with permission from McGraw-Hill, Inc.)

neously radar, aircraft, and other devices to observe the storms both remotely and *in situ*, were published in an important volume called *The Thunderstorm*.[207]

It was found that an individual storm ordinarily consists of a pattern of cells in various stages of development (Fig. 8.5). Cells in the early stages consist of vigorous updraft, in which hydrometeors are growing rapidly. Mature cells have both an active updraft and a downdraft, the latter coinciding with a downpour of precipitation. Dying cells contain only downdraft and precipitation that is still falling out. In *The Thunderstorm*, the term "thunderstorm" refers to the overall aggregate of cells, and its lifetime of several hours considerably exceeds that of an individual cell (~1 h). Thus, the pattern of cells within the multicell thunderstorm is continually changing.

Figure 8.6 illustrates the electrical structure of a multicell storm. An hypothetical but typical storm is shown at four successive times. At the first time (Fig. 8.6a), there are two mature cells in the storm. Each cell exhibits a distribution of charge similar to that shown in Fig. 8.3, with a region of negative charge at about the −15°C level sandwiched between the upper and lower positive regions. As in Fig. 8.4a, the initial lightning is intracloud and transfers negative charge to the upper positive region. In the multicell case, however, it is possible for some of the lightning to travel from the negative region of one cell to the upper positive region of a neighboring cell. At the second time (Fig. 8.6b), cloud-to-ground strikes have begun. As in the single-cell case (Fig. 8.2), these strikes come primarily after the initial period of intracloud lightning, and they again carry negative charge from the primary negative region to the earth's surface. These discharges may also have large horizontal components, which, as shown, can extend across the main negative regions of adjacent cells. At the third time (Fig. 8.6c), the anvil has become more extensive, and intracloud discharges penetrate into it from the main part of the storm. Cloud-to-ground discharges (not shown) are also sometimes observed to emanate from the anvil. Also by this time, one of the cells has dissipated and taken on the stratiform structure characteristic of this phase of the cell's development (Fig. 6.1b and Fig. 8.2). The shading in Fig. 8.6c and d shows the location of the melting layer and radar bright band. Balloon-borne electric field measurements in stratiform precipitation of extratropical cyclones and mesoscale convective

[207] This report was edited by H. R. Byers and R. R. Braham (1949). The Thunderstorm Project was directed by Professor Byers, then at the University of Chicago. Before the close of World War II, it had become clear that neither military nor commercial aviation could avoid flying in and around thunderstorms. To promote the safety of such aviation "information was needed concerning the internal structure and behavior of the thunderstorm." The project was therefore organized as a joint undertaking of the U.S. Air Force, Navy, the National Advisory Committee for Aeronautics, and the Weather Bureau. It took advantage of equipment and experienced personnel that were available in great numbers at the end of the war. Twenty-two freight cars full of ground equipment (not counting numerous trucks and jeeps) and ten Northrup P-61C "Black Widow" aircraft were made available to the program. Radar equipment, first used in the war and radiosonde equipment and surface instrumentation were deployed. Upon inquiring among "highly competent instrument pilots of the Air Force for volunteers for this work. ... The response was extremely gratifying and brought to the Project experienced crews, most of whom had served as instrument flight instructors." In addition, a group from the Soaring Society of America volunteered to make instrumented sailplane flights into thunderstorms for part of the program.

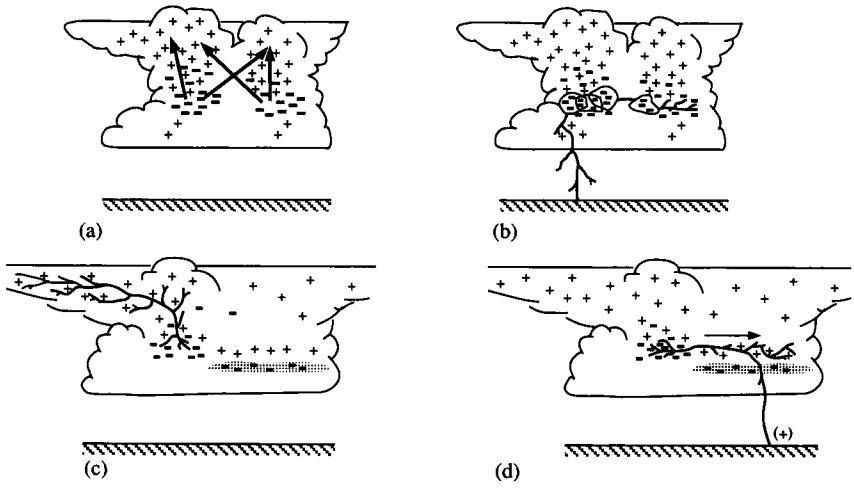

Figure 8.6

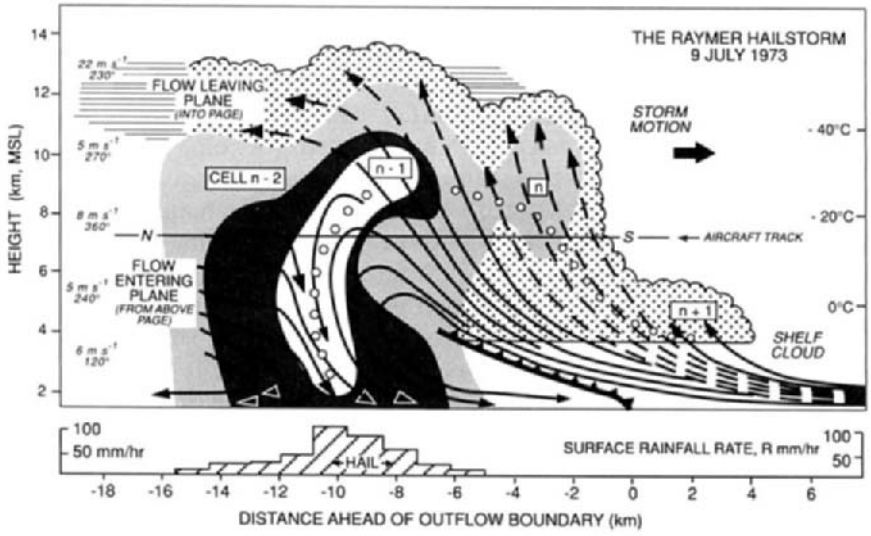

Figure 8.7

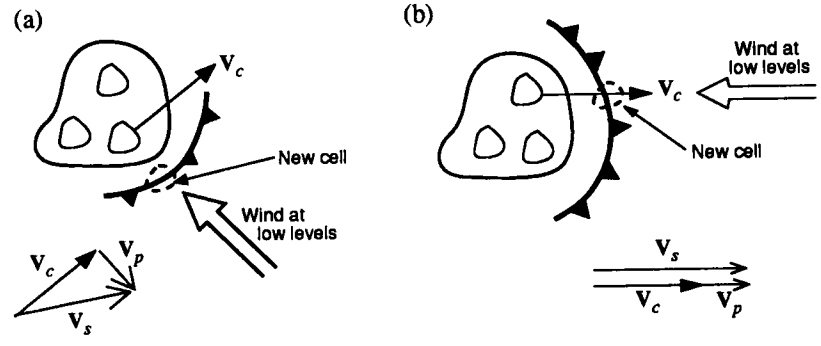

Figure 8.8

systems indicate that negative charge may accumulate in bright-band layers,[208] and this characteristic is postulated to apply in the melting layer of the dissipating cell of Fig. 8.6c and d. At the fourth time (Fig. 8.6d), horizontal intracloud lightning is occurring between the main negative area of the still-active cell and a region of positive charge at about the same level in the dissipating cell. These horizontal discharges are observed to occur repetitively at intervals of a few minutes or more. Occasionally, the dissipating cell can produce positive strokes to the ground that remove positive charge from this level.

Under certain conditions of wind shear (to be considered later in this chapter), a multicell thunderstorm takes on a form of organization illustrated in Fig. 8.7. The figure can be thought of either as an instantaneous picture of the storm, with cells in various stages of development, or as a sequence of stages in the life of one cell, which move, in a relative sense, through the storm. New cells (at $n + 1$ in Fig. 8.7) form on or just ahead of the leading edge of the storm. As cells move through the storm, they undergo their life cycles. At $n + 1$ and n, the cells are in the developing stage, with updraft air filling the cells and precipitation particles developing aloft but not yet falling to the ground. Precipitation particles are initiated near cloud base at $n + 1$ and grow by collection of cloud water. Above the 0°C level, the collectors are primarily ice particles, whose growth, after their formative stages, is dominated by the accumulation of rime ice. Continuation of this riming can build up graupel particles and hailstones, which eventually become big enough to fall relative to the ground. The schematic hail trajectory in the figure is one possibility based on an assumption that the particle, once initiated, remains

[208] Chauzy *et al.* (1980, 1985).

Figure 8.6 The apparent electrical structure and evolution of lightning in a multicell thunderstorm, as inferred from a variety of observations in different storms. A mature storm is illustrated in (a) and (b). A dissipating storm is depicted in (c) and (d). Branched structure of the lightning has been suggested in all cases except for the multicellular discharge shown in (a). The shaded region in (c) and (d) represents the radar bright band from melting snow. Positive and negative signs indicate the polarity of the charge at various locations. (From Krehbiel, 1986. Reprinted with permission from the National Academy Press, Washington, D.C.)

Figure 8.7 Schematic model of a multicell thunderstorm observed near Raymer, Colorado. It shows a vertical section along the storm's north-to-south (N–S) direction of travel, through a series of evolving cells. The solid lines are streamlines of flow relative to the moving system; they are broken on the left side of the figure to represent flow into and out of the plane and on the right side of the figure to represent flow remaining within a plane a few kilometers closer to the reader. The chain of open circles represents the trajectory of a hailstone during its growth from a small particle at cloud base. Lightly stippled shading represents the extent of cloud and the two darker grades of stippled shading represent radar reflectivities of 35 and 45 dBZ. The white area enclosing the hail trajectory is bounded by 50 dBZ. Environmental winds (m s^{-1}, deg) relative to the storm are shown on the left-hand side of the figure. (From Browning *et al.*, 1976. Reprinted with permission from the Royal Meteorological Society.)

Figure 8.8 Possible horizontal arrangements of cells in multicell thunderstorms. Solid contours indicate radar echoes of two different intensities. Frontal symbol denotes gust-front location. Vectors indicate the velocity of an individual cell ($\mathbf{V}_c$), storm propagation velocity resulting from new cell development ($\mathbf{V}_p$), and velocity of the storm as a whole ($\mathbf{V}_s$).

within the same cell throughout its lifetime. Other possible hail growth scenarios exist within multicell thunderstorms. For example, it has been suggested that optimal hail production in a multicell storm occurs by the initiation of graupel particles and hailstones in smaller cells and their subsequent advection into the updraft of the most intense cell of the storm.[209]

There are several horizontal configurations to which the organized multicellular vertical cross section in Fig. 8.7 can apply. The case in Fig. 8.8a, for example, shows cells forming systematically to the right of the cell-motion vector. This produces a right-moving thunderstorm. Similarly, the situation in Fig. 8.8b represents a forward-moving storm.

8.3 Supercell Thunderstorms

So far we have discussed only the single-cell and multicell thunderstorms, the latter being characterized by a fluctuating pattern of relatively short-lived cells. Another basic type of cumulonimbus structure is the *supercell thunderstorm*, which is far rarer and much more violent. Supercell thunderstorms are notorious for producing damaging hail and tornadoes. These storms could be the subject of much study because of their severe weather characteristics alone; however, further motivation is provided by the vorticity of the air in these storms. This vorticity, which gives rise to the tornadoes, is a fascinating manifestation of geophysical fluid dynamics, with many scientifically alluring facets. The name supercell[210] refers to the fact that although this type of storm is about the same size as a multicell thunderstorm, its cloud structure, air motions, and precipitation processes are dominated by a single storm-scale circulation consisting of one giant updraft–downdraft pair.

The exterior visual appearance of a supercell storm is sketched in Fig. 8.9 in the form that is usually taught to ground-based tornado spotters. The tornado vortex is visible as a funnel-shaped cloud pendent from a rotating wall cloud extending downward from the cloud base. Water condenses to form a cloud marking the funnel because of the lowering of the pressure in the intense vortex. To a first approximation, the vortex is cyclostrophic; hence, according to (2.46), the pressure decreases strongly inward toward the center of the vortex, in proportion to the square of the vortex wind speed. The tornado usually occurs near the peak of a wedge of low-level warm air, entering the region of the storm typically from the east or southeast. This warm air rises over the gust front to form the updraft of the storm-scale circulation. Dense downdraft air deposited by the storm at the surface spreads out behind the gust front. Precipitation reaching the ground behind the gust front forms a curved backdrop for the tornado. Weaker tornadoes can occur along the southwest (or rear-flank) gust front.

An idealized horizontal projection of the cloud-top topography of a supercell thunderstorm, as it would appear in a satellite picture, and the low-level precipita-

[209] See Heymsfield *et al.* (1980).

[210] Coined by Browning (1964).

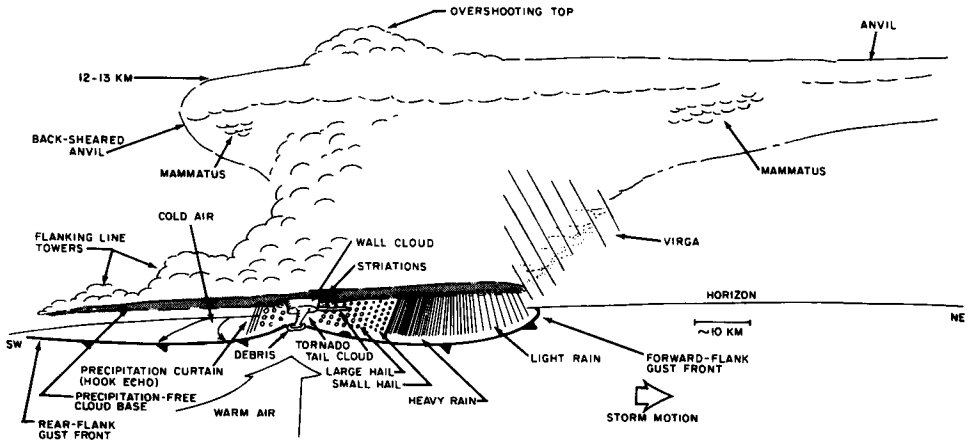

Figure 8.9 Schematic visual appearance of a supercell thunderstorm. (Based on U.S. National Severe Storms Laboratory publications and an unpublished manuscript of Howard B. Bluestein.)

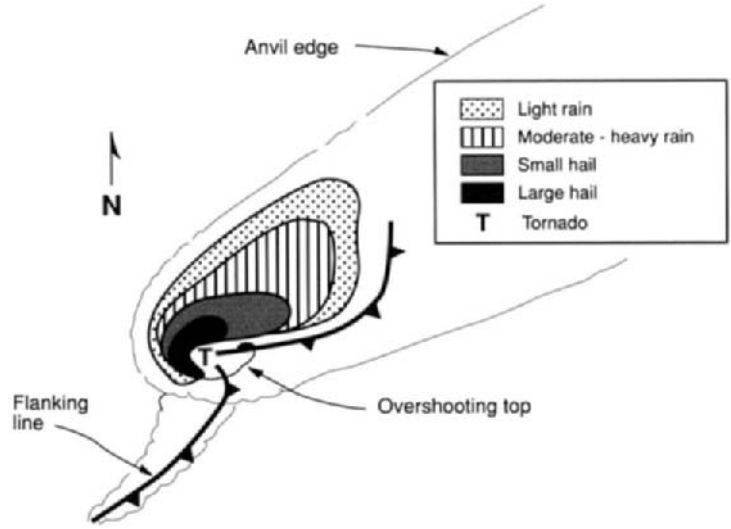

Figure 8.10 Idealized plan view of a supercell thunderstorm as it would appear in a satellite picture and in the low-level precipitation pattern that would be detected by a horizontally scanning radar. Cloud features seen by satellite include the flanking line, the edge of the anvil cloud, and the overshooting cloud top. Positions of the gust front (given by frontal symbols) and tornado are also shown. (Based on U.S. National Severe Storms Laboratory publications.)

tion pattern that would be detected by a horizontally scanning radar are shown superimposed in Fig. 8.10. The near coincidence of the tornado, the peak of the wedge of warm air, the overshooting cloud top, and the indentation in the horizontal precipitation area are evident. The horizontal distribution of precipitation at the ground is sorted according to particle size and thus produces a distinctive radar reflectivity pattern, since light rain, heavy rain, and small and large hail

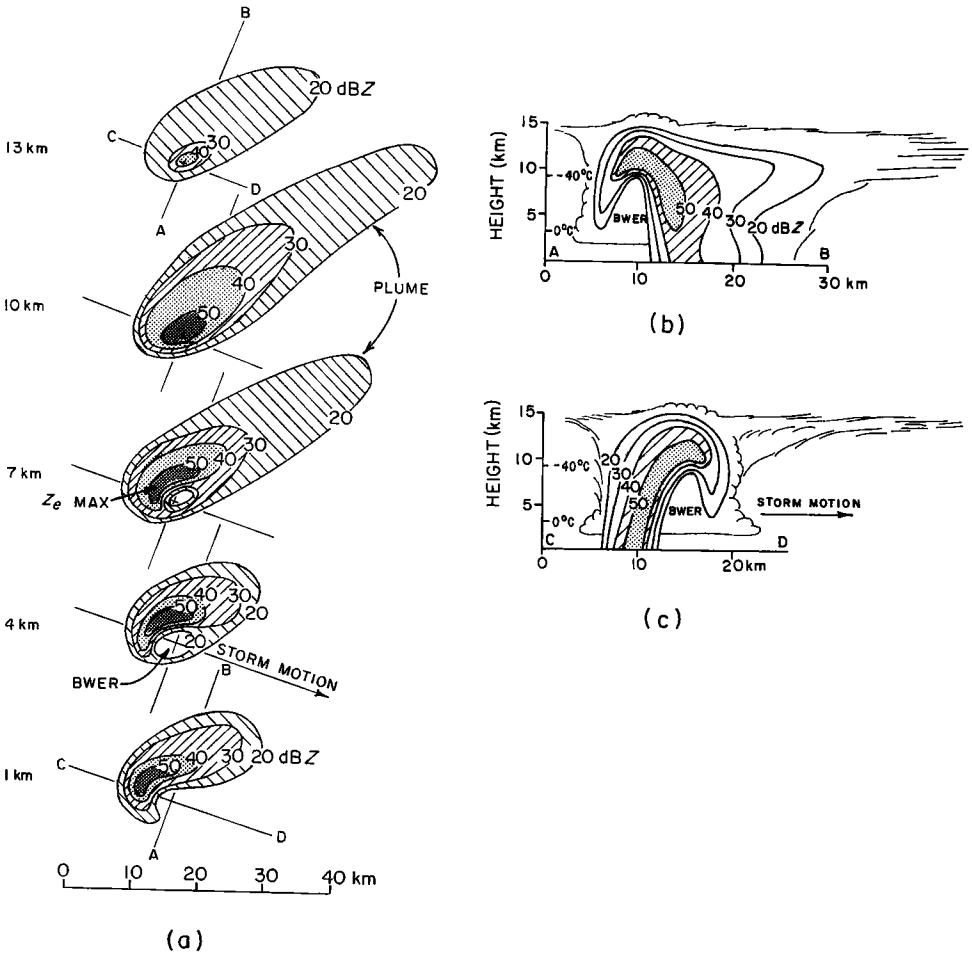

Figure 8.11 Schematic illustrating the variation of radar reflectivity patterns with height in supercell thunderstorms observed in Alberta, Canada. Horizontal sections of reflectivity (dBZ) at various altitudes are shown in (a). Vertical sections are shown in (b) and (c). Cloud boundaries are sketched. BWER refers to the bounded weak echo region. (From Chisholm and Renick, 1972.)

produce increasingly greater echo intensities. The large hail produces an extremely intense echo surrounding the notch in the precipitation pattern where the tornado is located. This radar reflectivity pattern is generally referred to as a *hook echo.*

The radar reflectivity patterns vary significantly with height in the storm (Fig. 8.11). The notch in the low-level horizontal echo pattern (1 km in Fig. 8.11a) is associated with a *bounded weak-echo region* (BWER) or *echo-free vault* that extends upward toward the overshooting top of the storm (Fig. 8.11a, 4 and 7 km; Fig. 8.11b and c).

The extremely strong updraft in the supercell thunderstorm (~10–40 m s^{-1})

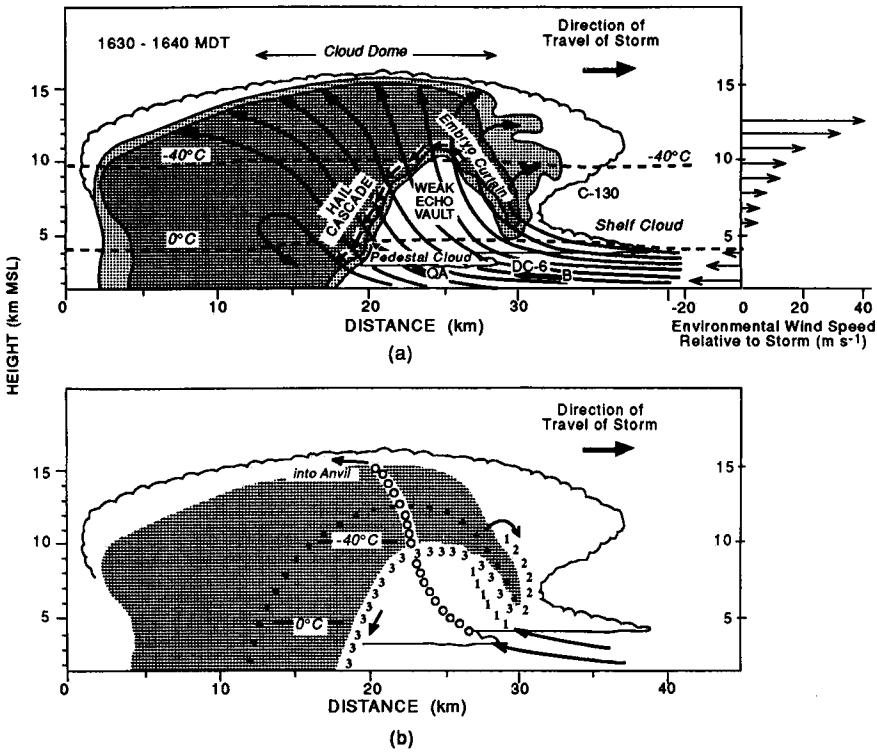

Figure 8.12 (a) Vertical cross section of cloud and radar echo structure of a supercell thunderstorm in northeastern Colorado. The section is oriented along the direction of travel of the storm, through the center of the main updraft. Two levels of radar reflectivity are represented by different densities of hatched shading. The locations of four instrumented aircraft are indicated by C-130, QA, DC-6, and B. Bold arrows denote wind vectors in the plane of the diagram as measured by two of the aircraft (scale is only half that of winds plotted on right side of diagram). Short thin arrows skirting the boundary of the vault represent a hailstone trajectory. The thin lines are streamlines of airflow relative to the storm. To the right is a profile of the wind component along the storm's direction of travel. (b) Vertical section coinciding with (a). Cloud and radar echo are the same as before. Trajectories 1, 2, and 3 represent three stages in the growth of large hailstones. The transition from stage 2 to stage 3 corresponds to the reentry of a hailstone embryo into the main updraft prior to a final up–down trajectory during which the hailstone may grow large, especially if it grows close to the boundary of the vault as in the case of the indicated trajectory 3. Other, less-favored hailstones will grow a little farther from the edge of the vault and will follow the dotted trajectory. Cloud particles growing within the updraft core are carried rapidly up and out into the anvil along trajectory 0 before they can attain precipitation size. (From Browning and Foote, 1976. Reprinted with permission from the Royal Meteorological Society.)

encourages the growth of very large hailstones. The growth process has been hypothesized to occur more or less as shown in Fig. 8.12. This figure illustrates the single, massive updraft, in which various hail trajectories can ensue, depending on the size and location of hail embryos when they first appear. The trajectories in the figure represent some plausible possibilities, given the observed radar reflectivity and air motion. Horizontal components of the trajectories, not shown

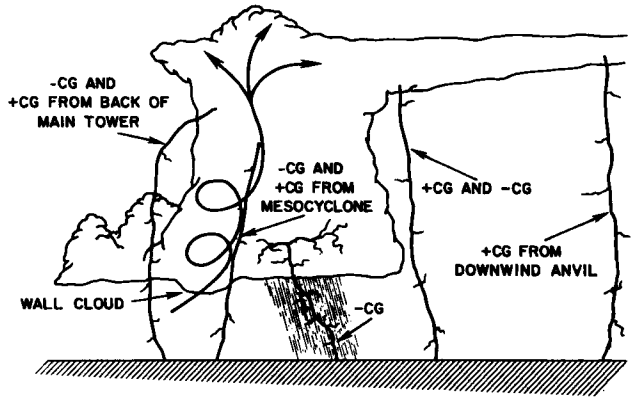

Figure 8.13 Sketch of observed locations and polarities of cloud-to-ground (CG) lightning flashes in supercell thunderstorms. The spiral (denoted mesocyclone) indicates the region of intense updraft and rotation. Only negative CGs have been observed in the precipitation core. The positive CGs seem to constitute only a very small percentage of the total flashes to ground. (From Rust *et al.*, 1981. Reprinted with permission from the American Meteorological Society.)

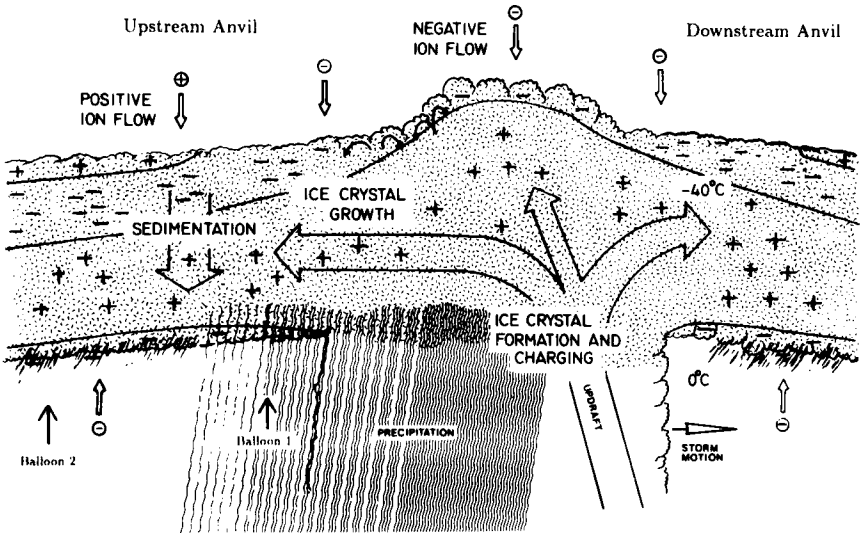

Figure 8.14 Conceptual model of the electrical structure in the upper levels of a supercell thunderstorm. Positive and negative signs indicate the polarity of the charge at various locations. Short curved streamlines at the top of the main cloud tower indicate turbulent mixing. Based on data obtained from two balloon sondes. (From Byrne *et al.*, 1989. © American Geophysical Union.)

here, can also be important to the growth of hail. The fallout of precipitation, as in all cumulonimbus, affects the downdraft for the supercell through precipitation drag and evaporation.

The supercell thunderstorm is also more active electrically than the single-cell or multicell thunderstorms. The overall lightning flash rate in supercells is ~10–40

min^{-1} overall and 5–12 min^{-1} for CG lightning. For more ordinary thunderstorms the overall rate is ~2–10 min^{-1}, while the CG rate is ~1–5 min^{-1}.[211] The observed spatial pattern of the cloud-to-ground lightning in the supercell is indicated in Fig. 8.13. In single-cell and multicell thunderstorms, positive CG strikes are associated with the dissipating cells (e.g., Fig. 8.6d). In the supercell, positive CG strikes occur in the mature as well as the dissipating stages of the storm. The positive strikes, however, account for only a small portion of the total number of strikes, and the lightning in the precipitation core is all negatively charged. Relatively little is known about the distribution of charge within the supercell thunderstorm. Measurements obtained in the anvil of one storm suggest the distribution of charge at upper levels shown in Fig. 8.14. Ice crystals transported up in the strong updraft are positively charged and are advected into both the forward and trailing anvil. This structure is not unlike the single-cell and multicell storm structures illustrated in Figs. 8.3 and 8.6. Atop the anvil is a complex double-layered screening zone.

8.4 Environmental Conditions Favoring Different Types of Thunderstorms

Whether a given thunderstorm turns out to be single-cellular, multicellular, or supercellular depends on both the wind shear and static stability of the environment. Three-dimensional numerical cloud models described in the last chapter (Sec. 7.5.3) have been particularly helpful in identifying the relationships between environmental conditions and the forms that thunderstorms take. The behavior of the model thunderstorms is related quantitatively to the stability and shear as follows.[212]

The buoyant stability of the environment can be represented by the *convective available potential energy (CAPE)*, which is given by

$$\text{CAPE} \equiv g \int_{\text{LFC}}^{z_T} \frac{\theta(z) - \bar{\theta}(z)}{\bar{\theta}(z)}\, dz \tag{8.1}$$

where θ is the potential temperature of a parcel of air lifted from $z = 0$ to $z = z_T$ while not mixing with its environment. The parcel rises dry adiabatically [conserving its θ, according to (2.11)] until it becomes saturated and then rises moist adiabatically [conserving its θ_e, according to (2.18)] thereafter. $\bar{\theta}$ is the potential temperature of the environment (base state), the LFC (level of free convection) is the height at which the parcel becomes warmer than the environment, and the cloud top z_T is assumed to be the level where $\theta = \bar{\theta}$.[213]

[211] These rates were reported by Rust *et al.* (1981).

[212] This discussion is based on the work of Weisman and Klemp (1982).

[213] Synoptic meteorologists will recognize CAPE as the net *positive area* on a pseudoadiabatic chart. The positive area is the area between the parcel and environment temperature on a chart with temperature as the abscissa and height (or log pressure) as the ordinate and the scales adjusted so that the positive area is proportional to energy.

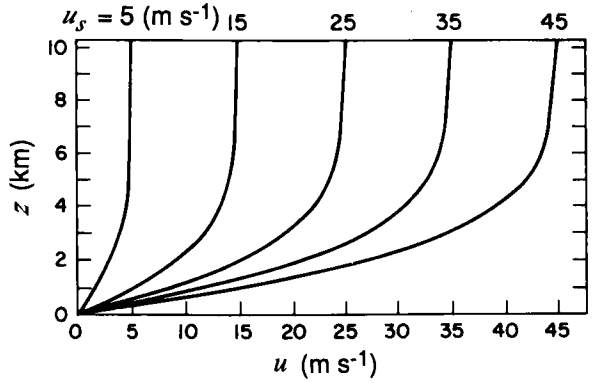

Figure 8.15 Profiles of wind speed u used in three-dimensional model simulations of multicell and supercell thunderstorms. Profiles becomes asymptotic to u_s. (From Weisman and Klemp, 1982. Reprinted with permission from the American Meteorological Society.)

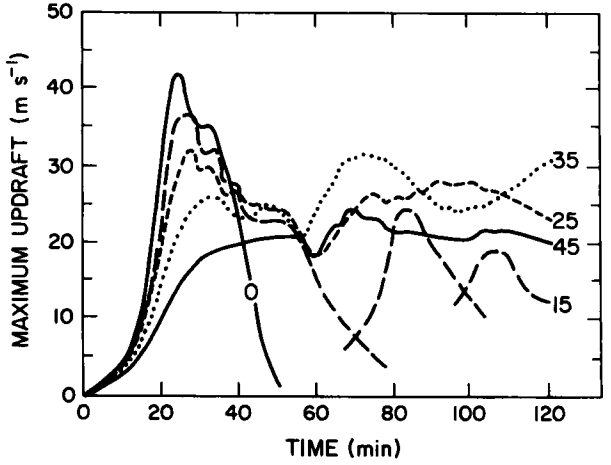

Figure 8.16 Results of three-dimensional model simulations of thunderstorms under different amounts of wind shear. The quantity plotted is the maximum vertical velocity as a function of time for different values of the wind-shear parameter u_s(m s^{-1}), which is the number plotted next to each curve. (From Weisman and Klemp, 1982. Reprinted with permission from the American Meteorological Society.)

The wind shear in an idealized environment can be represented by the asymptotic wind speed u_s, reached at the height z_s, the top of a shear layer, in an hypothetical environment in which the wind is unidirectional with magnitude,

$$u = u_s \tanh(z/z_s), \quad z_s = 3 \text{ km} \tag{8.2}$$

Examples of this wind profile are shown in Fig. 8.15.

Model results are illustrated in Fig. 8.16 for an environment whose $\bar{\theta}$ increases with height such that the environmental saturated equivalent potential tempera-

ture $\bar{\theta}_{es}$ [as defined in (2.146)] is constant.[214] Different values of $\theta(z)$ were tried in (8.1) for a parcel lifted from $z = 0$ by letting the surface humidity take on various values while keeping the surface temperature constant. The results in Fig. 8.16 are for a surface mixing ratio of 14 g kg^{-1}, a surface temperature of about 23°C, and the various wind profiles shown in Fig. 8.15. The model convection was initialized as a buoyant bubble 10 km in horizontal radius, 1.4 km in vertical radius, and 2°C in temperature excess at its center. Three different model responses were seen, depending on the strength of the environmental shear. Figure 8.16 shows the maximum vertical velocity as a function of time for different values of u_s. For zero shear, a single-cell storm occurred ($u_s = 0$). For moderate shear ($u_s = 15$ m s^{-1}), a sequence of cells occurred, indicating multicellular storm structure. For strong shear ($u_s = 25$, 35, and 45 m s^{-1}), a single cell reached a plateau of vertical velocity and continued to be maintained through a process of redevelopment. This redevelopment, as we will see, is a characteristic of rotational supercell dynamics.

The structure of the model multicell storm obtained under moderate shear is illustrated by the superimposed low-level flow and midlevel vertical velocity in Fig. 8.17. After 40 min (Fig. 8.17a), the initial updraft (cell 1) had weakened, and cold outflow had pushed 10 km ahead of the updraft core. The updraft was thus cut off from inflow of warm air, and the maximum convergence was located at the gust front well ahead of the old updraft core. This convergence produced a new updraft (cell 2), which was ahead of cell 1 after 80 min (Fig. 8.17b). By 120 min (Fig. 8.17c), the updrafts of cells 1 and 2 had disappeared, but a third cell had formed at the gust front when the updraft of cell 2 was cut off from the inflow. Noteworthy is the consistency of this storm, with its sequential cell development, and the empirical multicell storm structure pictured in Fig. 8.7.[215]

Some characteristics of the model supercell storm obtained when the environment had higher shear are shown in Fig. 8.18, which, like Fig. 8.17, shows only half of the model domain. Since the wind shear of the environment is unidirectional, the results are symmetric about the axis $y = 0$. It is particularly important to note this symmetry in the supercell case, because two identical storms develop and move away from the y-axis. This process is referred to as *storm splitting* and is intrinsic to supercell dynamics. The storm that moves to the right of the y-axis (shown in the figure) is called the *right-moving* storm. The other member of the split (not shown) is called the *left-moving* storm. In this mode, the gust front does not outrun the updraft core. Instead, they move together in a state of near equilibrium, in which the rates of cold outflow and warm inflow are about equally matched. The movement of the updraft core away from the y-axis is a result of the rotational dynamics of the storm, which are particularly robust when the environmental shear is strong. The symmetrical behavior of storm splitting, in which left- and right-moving storms occur as mirror images of each other, is the result of unidirectional wind shear. We will see that if the direction as well as the speed of

[214] Such an environment is referred to as *moist adiabatic*.

[215] The behavior of the multicell storm, whereby the downdraft outflow moves so fast that it outruns the existing updraft cell and forms a new cell at the gust front, had been pointed out in an earlier modeling study by Thorpe and Miller (1978).

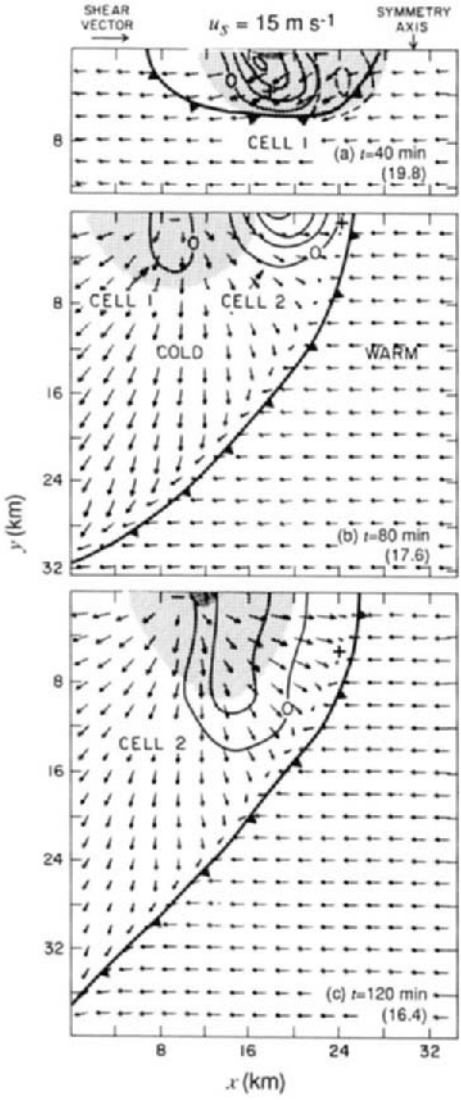

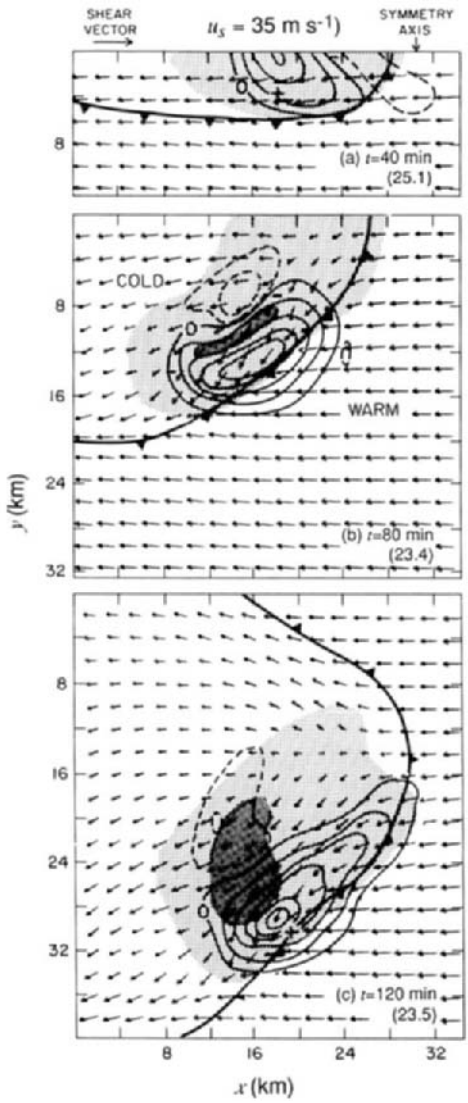

Figure 8.17

Figure 8.18

Figure 8.17 Results of a model simulation showing a multicell thunderstorm occurring under conditions of moderate environmental wind shear (u_s = 15 m s^{-1}). Fields are shown for three times during the simulation. Vectors represent storm-relative wind at an altitude of 178 m. The maximum vector magnitude (m s^{-1}) is shown in parentheses in the lower right corner of each plot. The surface rain field is indicated by stippling. The surface gust front is denoted by the frontal symbol and corresponds to the −0.5°C temperature perturbation contour. The midlevel (4.6 km) vertical velocity field is contoured every 5 m s^{-1} for positive values and 2 m s^{-1} for negative values. The zero contours outside the main region of storm activity have been deleted. Plus and minus signs represent the location of the low-level (178 m) vertical velocity maximum and minimum, respectively. Only the southern half of the model domain is shown. The fields in the northern half are mirror images. (From Weisman and Klemp, 1982. Reprinted with permission from the American Meteorological Society.)

Figure 8.18 Results of a model simulation showing a supercell thunderstorm occurring under conditions of strong environmental wind shear (u_s = 35 m s^{-1}). Format same as Fig. 8.17. (From Weisman and Klemp, 1982. Reprinted with permission from the American Meteorological Society.)

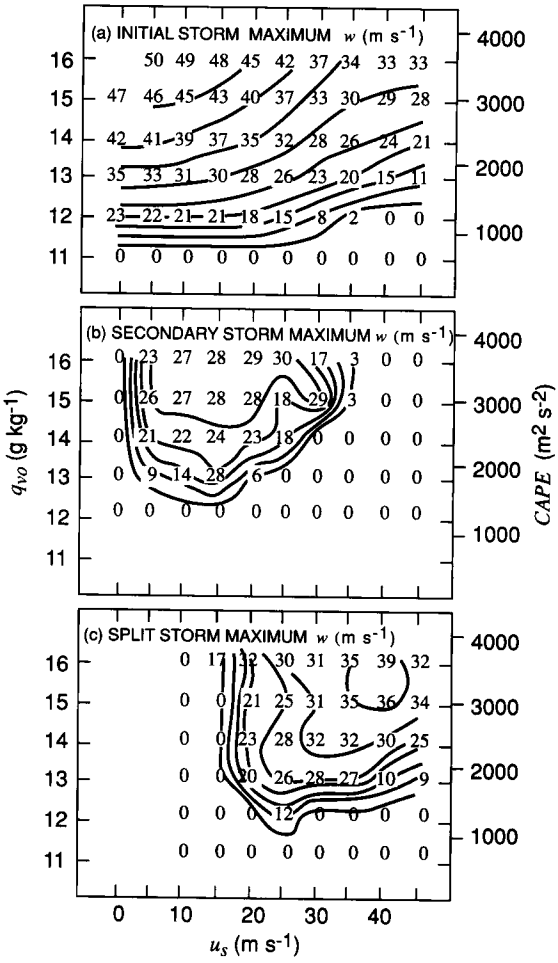

Figure 8.19 Maximum vertical velocity of model thunderstorms as a function of CAPE and wind-shear parameter u_s. Panels (a) and (b) refer to multicell cases; panel (c) refers to supercell cases. (From Weisman and Klemp, 1982. Reprinted with permission from the American Meteorological Society.)

the wind in the environment varies with height, either the left- or the right-moving storm is favored, while the other is disfavored.

Further insight into the modes of thunderstorm organization is gained by plotting the maximum vertical velocity as a function of CAPE and u_s. Figure 8.19 shows results for multicell cases. To exist, the initial cell, as would be expected, must have a threshold amount of thermodynamic instability (Fig. 8.19a). Its intensity increases with increased instability and decreases with increased shear, as a result of enhanced entrainment favored by the shear. (Recall from Sec. 7.4.3 that the counter-rotating vortices produced by the tilting of the environmental shear near the convective updraft are an important mechanism by which midlevel air is entrained into the updraft.) From Fig. 8.19b, it is evident that a second cell will not

occur if there is no shear in the environment (i.e., the degenerate case of a single-cell thunderstorm occurs when there is too little shear to allow low-level inflow to match the downdraft spreading at the surface; consequently, a new cell cannot become established). When a secondary cell forms, the vertical velocity reaches a peak at low to moderate shear, where an approximate balance between inflow and outflow allows a new cell to form. When the shear becomes too strong, the new cell cannot be maintained against entrainment. The supercell cases (Fig. 8.19c) can occur only at moderate to high shear. The maxima in Fig. 8.19b and c indicate a bimodal distribution of thunderstorm type. The values of shear supporting a supercell are too high to support a secondary cell in a multicell storm. However, at the higher values of shear, internal rotation becomes stronger. Associated with the rotation are dynamic pressure perturbations. The dynamically induced pressure field, in turn, affects the movement of the storm, accounting for storm splitting and right- and left-moving storm propagation. We will now explore these and other topics associated with the rotational dynamics of the supercell thunderstorm in more detail.

8.5 Supercell Dynamics[216]

8.5.1 Storm Splitting and Propagation

The initial storm splitting and propagation of the two updraft cores of a supercell away from the along-shear axis in an environment of unidirectional shear were illustrated three-dimensionally in Fig. 7.23. The first panel shows the vortex couplet that arises when the horizontal vorticity associated with the environmental shear is tilted by the updraft. The second panel shows the storm after splitting has occurred.

Crucial to understanding the split is that both vortices contain a pressure perturbation minimum. The nature of this minimum can be seen by considering again the diagnostic equation for the pressure perturbation (7.4) and recalling that the pressure perturbation can be split into partial pressures p_B^* and p_D^*, associated with buoyancy and dynamic sources, respectively. The vertical component of the equation of motion (7.2) can then be written

$$\frac{\partial w}{\partial t} = -\frac{1}{\rho_o}\frac{\partial p_D^*}{\partial z} - \left(\frac{1}{\rho_o}\frac{\partial p_B^*}{\partial z} - B\right) - \mathbf{v}\cdot\nabla w \tag{8.3}$$

Numerical-model calculations show that the terms in parentheses tend to balance. Substituting (7.6) into (7.9) and making use of the anelastic continuity equation (2.54) leads to

$$\begin{aligned}\nabla^2 p_D^* &= -\nabla\cdot\left(\rho_o \mathbf{v}\cdot\nabla\mathbf{v}\right)\\ &= -\rho_o\left(u_x^2 + v_y^2 + w_z^2 - \frac{d^2\ln\rho_o}{dz^2}w^2\right) - 2\rho_o\left(v_x u_y + u_z w_x + v_z w_y\right)\end{aligned} \tag{8.4}$$

The first term in the last parentheses is dominant in locations in the thunderstorm occupied by strong vortices. In the case of a purely rotational horizontal flow, for

[216] The discussion in this section closely follows the review article of Klemp (1987).